

Supporting Information

Designed growth of tungsten-doped nickel oxide nanocrystal film toward high electrochromic performance with neutral color

Feiyue Yao,^{a,b} Yong Zhang,^{* a,b} Jingzhi Li,^{a,b} Shangzhi Yao,^{a,b} Xueru Zhang,^{b,c}
Jiewu Cui,^{a,b} Yan Wang,^{a,b} Jiaqin Liu^d and Yucheng Wu^{* a,b}

a. School of Materials Science and Engineering, Hefei University of Technology, Hefei 230009, Anhui, China

b. Key Laboratory of Advanced Functional Materials and Devices of Anhui Province, Hefei 230009, China

c. Instrumental Analysis Center, Hefei University of Technology, Hefei 230009, China

d. College of Chemistry, Beijing University of Chemical Technology, Beijing 100029, China

Email address: zhangyong.mse@hfut.edu.cn (Yong Zhang), ycwu@hfut.edu.cn (Yucheng Wu)

Tel: **Yong Zhang : 86-551-62905152

Experimental section

Materials

All reagents were prepared for use and did not require any further purification. Nickel acetylacetonate ($\text{Ni}(\text{acac})_2$), oleylamine, 1,3,5-trimethylbenzene, and lithium perchlorate were purchased from Aladdin. Toluene, n-hexane, acetone, and anhydrous ethanol were acquired from Sinopharm Reagent. Propylene carbonate (PC) was purchased from McLean's Reagent. The FTO glass was procured from South China Hunan City Technology Co., Ltd. The pure tungsten target was acquired from Zhongnuo New Material (Beijing) Technology Co., Ltd.

Characterization

Structural characterization was studied by transmission electron microscopy (TEM, JEM-1400 flash) and field emission transmission electron microscopy (FETEM, JEM-2100F). Surface morphology was analyzed by high-resolution scanning electron microscopy (FESEM, Regulus 8230) and atomic force microscopy (AFM, Dimension Icon). X-ray photoelectron spectroscopy (XPS, ESCALAB250Xi) was performed using a spectrometer. Electrochemical properties were measured by an electrochemical workstation (CHI760E) and three-electrode system, where the electrolyte was 1M LiClO_4/PC , the reference electrode was Ag/AgCl, the counter electrode was Pt wire, and area of the working electrode was $3 \times 0.6 \text{ cm}^2$. The optical transmittance was measured in the wavelength range of 400-1000 nm by UV-visible near-infrared spectrophotometer (UV 3600).

Supporting Equations

Equation S1. Formula of optical modulation

$$\Delta T = T_b - T_c \quad (1)$$

Equation S2. Rayleigh scattering theory:

$$I_s = \frac{8\pi^4 M a^6}{\lambda^4 r^2} \left| \frac{n^2 - 1}{n^2 + 2} \right|^2 (1 + \cos^2 \theta) I_i \quad (2)$$

If the incident light is unpolarized, the irradiance is denoted by I_i and the scattered irradiance by I_s . The relevant parameters in this context are as follows: M is the number of particles, r is the distance from the observation point to the particles, θ is the scattering angle, n is the refractive index, and a is the radius of the particles.

Supporting Tables

Table S1. The roughness average (R_a) and the root mean square roughness (R_q) of NiO NCs film and W-NiO NCs film

Sample	R_a (nm)	R_q (nm)
NiO	5.40	6.74
W-NiO	4.74	6.03

Table S2. Transmittance of bleached NiO films compared to peers

Method	Modification strategy	Electrolyte	U_b (V) (vs. Ag/AgCl)	Wavelength (nm)	T_b (%)	Ref.
Chemical bath deposition	Mn doped NiO NSs	1 M KOH	-0.5	550	88%	1
Solvothermal	NiO NCs	1 M LiClO ₄ /PC	-1.5	550	87%	2
DC + RF magnetron sputtering	Li-Ta co-doped NiO NPs	1 M LiClO ₄ /PC	-1.0	550	85%	3
RF magnetron sputtering	WO ₃ doped NiO NRs	1 M LiClO ₄ /PC	-1.4	550	85%	4
Chemical spray pyrolysis	Zr doped NiO NPs	1 M KOH	-2.0	550	82%	5
Sol-Gel	N doped porous NiO	1 M KOH	0	450	82%	6
Pulsed magnetron sputtering	NiO nanopyramid film	1 M LiClO ₄ /PC	-1.0	550	80%	7
DC magnetron sputtering	NiO NRs	1 M LiClO ₄ /PC	-3.0	550	75%	8
Solvent thermal	Sn doped NiO NPs	0.5 M KOH	-0.6	550	70%	9
Solvent thermal	PYS-NiO NSs	1 M KOH	-0.6	592	58%	10
Solvent thermal & DC magnetron sputtering	W doped NiO NCs	1 M LiClO ₄ /PC	-0.5	550	95%	This work

Table S3. Chromatogram and transmittance of NiO NCs film and W-NiO NCs film

Samplpe	State	L*	a*	b*	T _b (%)	T _c (%)	ΔT (%)
NiO	bleached	71.34	-1.40	2.85	87.68	36.18	51.50
	colored	43.93	2.82	5.85			
W-NiO	bleached	74.30	-2.64	0.83	94.58	28.97	65.61
	colored	40.80	3.76	8.27			
FTO	–	85.53	-2.06	-2.60	100	–	–

In the CIE chromaticity coordinate space, the L* represents the brightness, ranging from 0 to 100. The a* represents the red-green axis, with more positive values representing red and negative values representing green. The b* represents the yellow-blue axis, with more positive values representing yellow and more negative values representing blue.

Table S4. Corresponding values of the XPS patterns of the NiO NCs film and W-NiO NCs film

Sample	Element	Atomic (%)	Assignment	Binding energy (eV)	FWHM (eV)	Atomic (%)
NiO	Ni	46.48	2p _{3/2} Ni ²⁺	853.62	1.18	2.29
			2p _{3/2} Ni ³⁺	855.28	3.01	6.20
	Ni	42.15	2p _{3/2} Ni ²⁺	854.06	1.28	2.39
			2p _{3/2} Ni ³⁺	855.70	2.87	5.76
W-NiO	W	2.93	4f _{7/2} W ⁵⁺	33.68	1.29	0.12
			4f _{5/2} W ⁵⁺	35.80	1.29	0.19
			4f _{7/2} W ⁶⁺	35.09	1.16	1.33
			4f _{5/2} W ⁶⁺	37.25	1.16	1.29

Table S5. Comparison of the optical properties after cycling

Samplpe	Number	State	L*	a*	b*	T _b (%)	T _c (%)	ΔT (%)
NiO	2500	bleached	72.63	-2.78	2.33	88.05	50.17	37.88
		colored	54.13	1.48	5.22			
W-NiO	5000	bleached	73.88	-2.79	1.01	92.17	34.34	57.83
		colored	43.15	3.49	7.78			
FTO	–	–	85.53	-2.06	-2.60	100	–	–

Supporting Figures

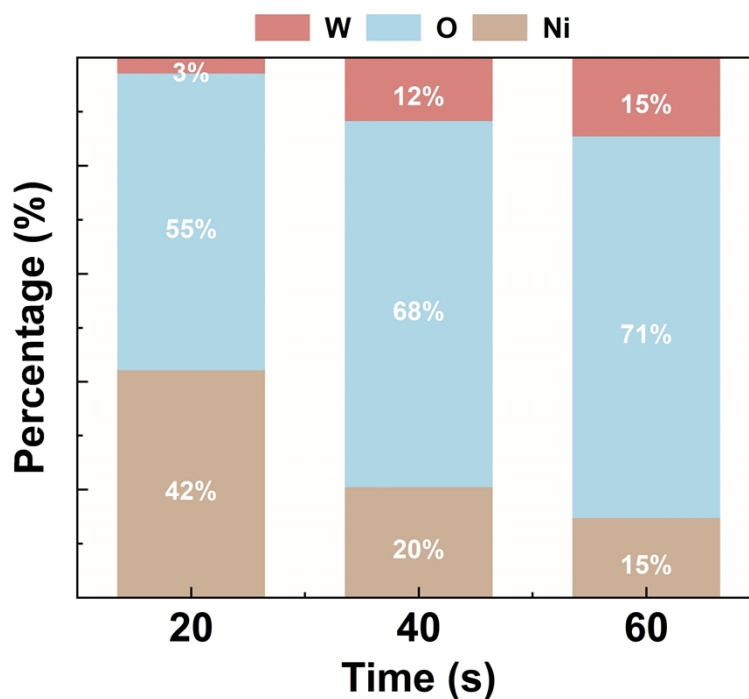


Fig. S1. Elemental content for different sputtering time

By adjusting the sputtering time, we explored the effect of different W concentrations on the electrochromic performance. XPS was used to measure the composition of films corresponding to different sputtering time (Fig. S1). With the extension of sputtering time, the W content in the NiO films gradually increased.

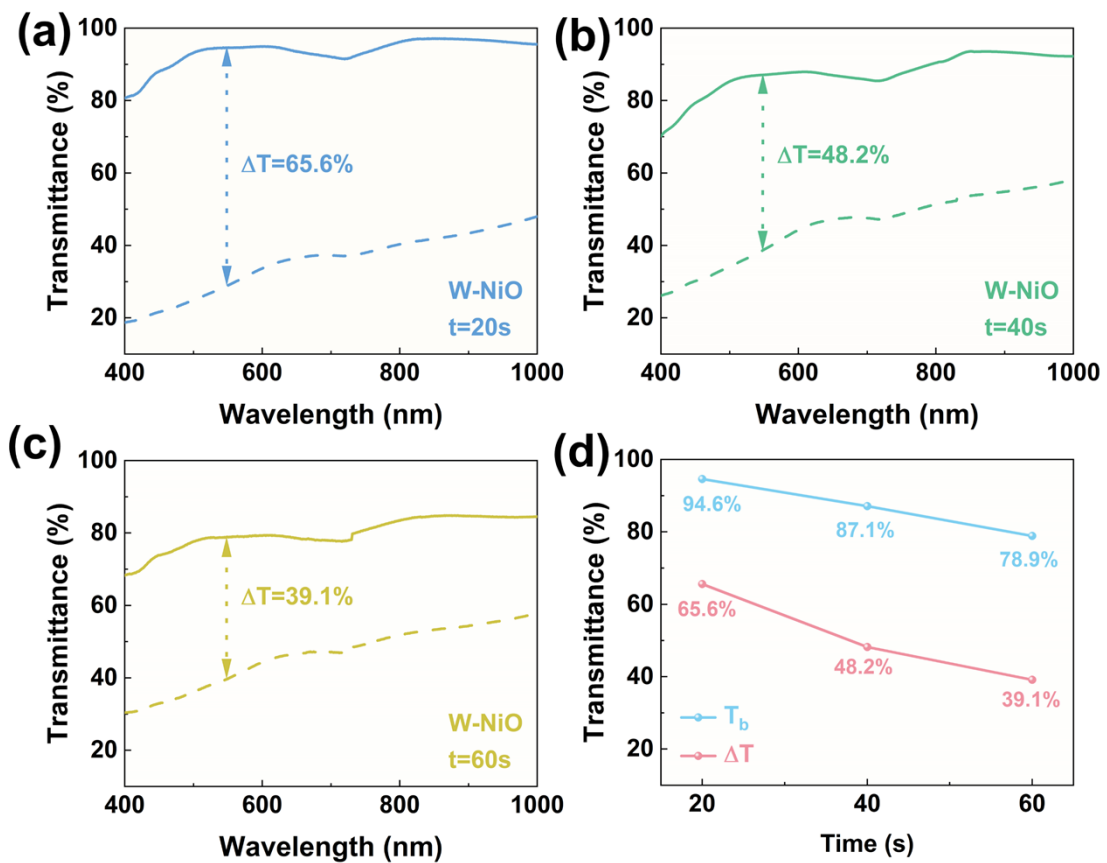


Fig. S2. Spectra of NiO films corresponding to different sputtering time

From 20s to 60s, both the optical modulation amplitude and the transmittance in the bleached state gradually decreased (Fig. S2 (a)-(d)), which indicates excessive W accumulation on the surface of the W-NiO film and hinders the insertion and extraction of Li^+ ions, ultimately leading to poor performance.

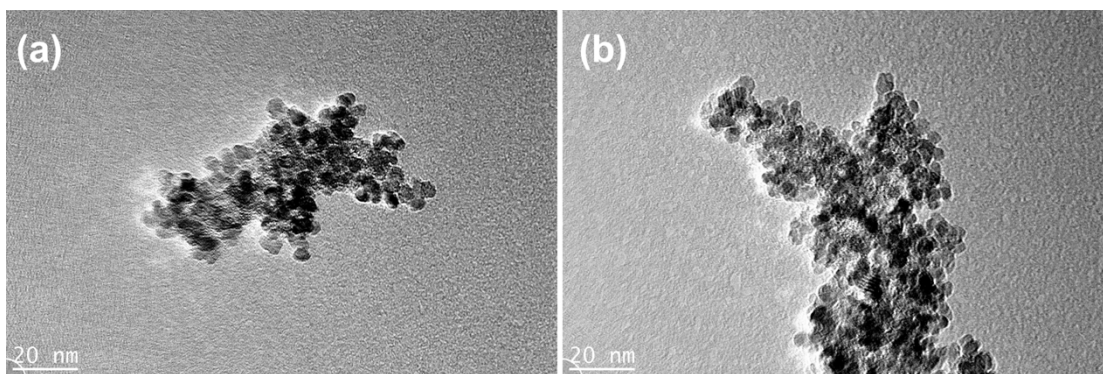


Fig. S3 (a) and (b) FETEM images of NiO NCs

To determine the size of the nanocrystals, the film was scraped from the FTO substrate followed by dispersing the powder film in a toluene solution. After sonication, the nanoparticle size distribution image was obtained as shown in Fig. S3 (a) and (b).

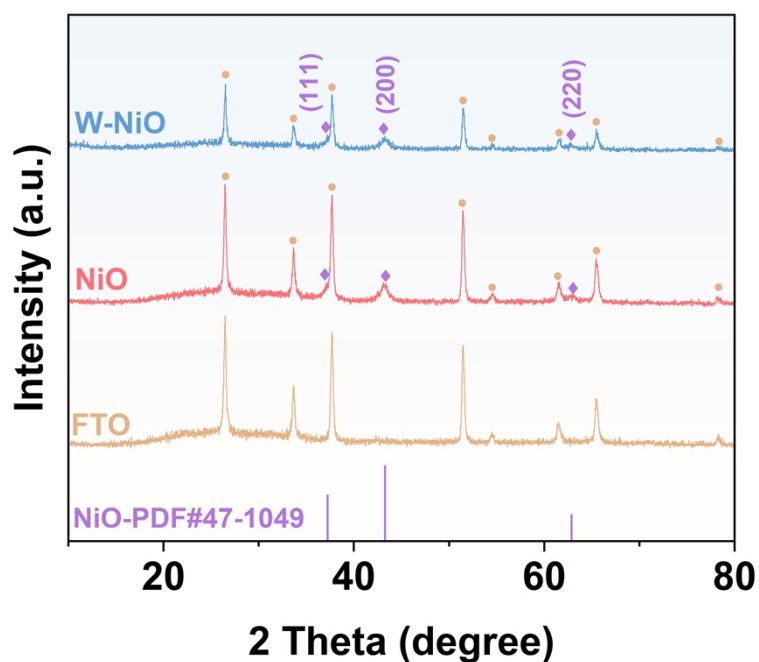


Fig. S4. XRD pattern of NiO and W-NiO in FTO glass

Due to the deposition on FTO, characteristic peaks corresponding to FTO are prominently observed. The diffraction peaks of NiO NCs are compared with the standard (JCPDS # 47-1049), and indexed as (200), (111), and (220) of the face-centered cubic (FCC) NiO structure, which demonstrates the high crystallinity of NiO NCs.¹¹ After the W doping, the diffraction peaks still correspond to the FCC NiO, indicating well-maintenance of the phase structure.

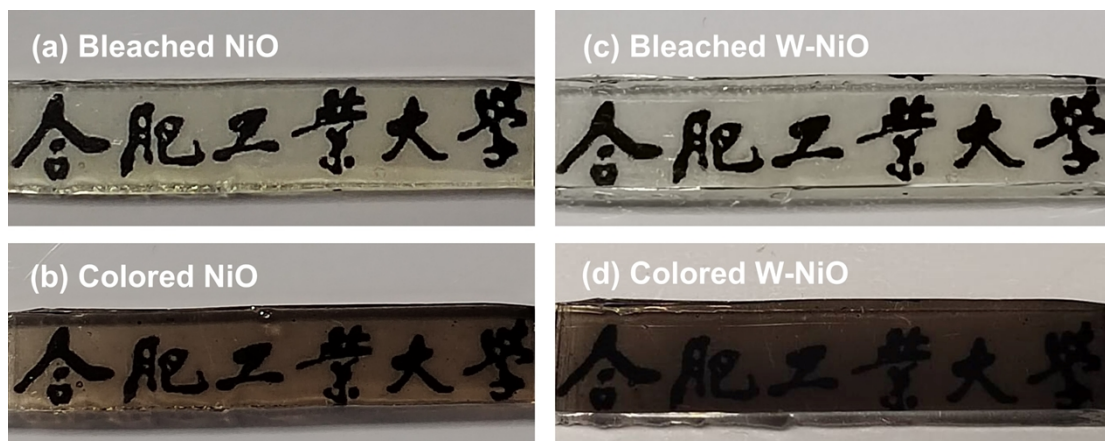


Fig. S5. Discoloration images of the films before and after the W doping

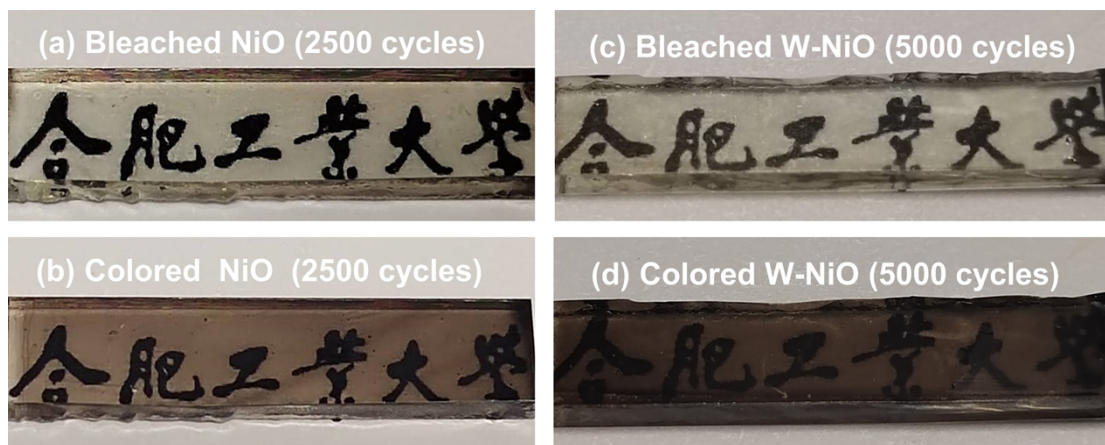


Fig. S6. Discoloration images of the films before and after the cycling process

As shown in **Fig. S6**, the electrochromic films did not peel after thousands of cycles, indicating the superior adhesion between the films and the FTO glass substrate.

References

- 1 L. Zhao, Y. Zhu, X. Long, W. Liao, B. Hu, R. Miao, G. Zhang, G. Sun, Y. Xie and L. Miao, *Ceram. Int.*, 2024, **50**, 12810-12817.
- 2 Z. Xie, Q. Liu, B. Lu, J. Zhai and X. Diao, *Mater. Today Commun.*, 2019, **21**, 100635.
- 3 Q. Huang, Q. Zhang, Y. Xiao, Y. He and X. Diao, *J. Alloys Compd.*, 2018, **747**, 416-422.
- 4 K. S. Usha and S. Y. Lee, *J. Alloys Compd.*, 2024, **1009**, 176774.
- 5 Y. Tian, H. Wang, S. Liu and B. Zhang, *Electrochim. Acta*, 2024, **506**, 145057.
- 6 K. Kim, S. Jeong, B. Koo and H. Ahn, *Appl. Surf. Sci.*, 2021, **537**, 147902.
- 7 Y. Shi, Y. Zhang, Y. Zheng, K. Tang, X. Ke, Z. Li, J. Tang, Z. Hui and L. Ye, *Ceram. Int.*, 2024, **50**, 55839-55844.
- 8 C. Zhang, Z. Li, Q. Zheng, X. Zhou, Z. Lin, J. Zhang, X. Tang, Y. Zhan and J. Luo, *Sol. Energy Mater. Sol. Cells*, 2024, **267**, 112729.
- 9 J. Hou, L. Gao, X. Gu, Z. Li, M. Huang and G. Su, *Mater. Chem. Phys.*, 2023, **306**, 128079.
- 10 B. Wang, Y. Huang, S. Zhao, R. Li, D. Gao, H. Jiang and R. Zhang, *Particuology*, 2024, **84**, 72-80.
- 11 Q. Huang, J. Wang, H. Gong, Q. Zhang, M. Wang, W. Wang, J. P. Nshimiyimana and X. Diao, *J. Mater. Chem. A*, 2021, **9**, 6451-6459.